Role of Anions in the $AuCl_3$-Doping of Carbon Nanotubes

Soo Min Kim,[†] Ki Kang Kim,[‡] Young Woo Jo,[†] Min Ho Park,[§] Seung Jin Chae,[†] Dinh Loc Duong,[†] Cheol Woong Yang,[§] Jing Kong,[‡,*] and Young Hee Lee[†,*]

[†]BK21 Physics Division, Department of Energy Science, and Center for Nanotubes and Nanostructured Composites, Sungkyunkwan Advanced Institute of Nanotechnology, Sungkyunkwan University, Suwon 440-746, Korea, [‡]Department of Electrical Engineering and Computer Sciences, Massachusetts Institute of Technology, Cambridge, Massachusetts 02139, United States, and [§]School of Advanced Materials Science and Engineering, Sungkyunkwan University, Suwon 440-746, Korea

ABSTRACT The doping/dedoping mechanism of carbon nanotubes (CNTs) with $AuCl_3$ has been investigated with regard to the roles of cations and anions. Contrary to the general belief that CNTs are p-doped through the reduction of cationic Au^{3+} to Au^0, we observed that chlorine anions play a more important role than Au cations in doping. To estimate the effects of Cl and Au on CNTs, the CNT film was dedoped as a function of the annealing temperature (100−700 °C) under an Ar ambient and was confirmed by the sheet resistance change and the presence of a G-band in the Raman spectra. The X-ray photoelectron spectroscopy (XPS) analysis revealed that the doping level of the CNT film was strongly related to the amount of adsorbed chlorine atoms. Annealing at temperatures up to 200 °C did not change the amount of adsorbed Cl atoms on the CNTs, and the CNT film was stable under ambient conditions. Alternatively, Cl atoms started to dissociate from CNTs at 300 °C, and the stability of the film was degraded. Furthermore, the change in the amount of Cl atoms in CNTs was inversely proportional to the change in the sheet resistance. Our observations of the Cl adsorption, either directly or mediated by an Au precursor on the CNT surface, are congruent with the previous theoretical prediction.

KEYWORDS: carbon nanotube · doping · $AuCl_3$ · sheet resistance · conductivity

Doping in carbon nanotubes (CNTs) has been a serious scientific and technological issue in transistor applications.[1−4] There are two current approaches to CNT doping. One approach is to dope CNTs during synthesis through the introduction of foreign atoms, such as boron (p-type doping) or nitrogen (n-type doping), allowing substitutional or interstitial impurities to be formed in the carbon network.[5] This method is similar to that adopted in conventional semiconductor technology. Nevertheless, the CNT situation is different because all of the atoms are exposed to the environment. For instance, unstable nitrogen atoms located at the surface can be easily oxidized under ambient conditions such that they no longer behave as an n-type dopant.[6−8] The second approach is to dope CNTs after synthesis. In this regard, ion bombardment has been attempted using n- or p-type ionic dopants. This method is technologically relevant; however, oxidation problems occur when samples are exposed under ambient conditions.[9] One method which utilizes this postsynthesis doping is a chemical approach that involves chemical adsorption to the CNT surface, perhaps the most relevant technique for producing a prominent doping effect on CNTs.

Chemical doping in CNTs involves charge transfer between the adsorbates and the nanotubes.[10] Several dopants have been introduced to dope CNTs using this technique. For instance, $AuCl_3$, $SOCl_2$, and $NOBF_4$ were used as p-type dopants in which electrons were extracted from CNTs into the adsorbates, whereas viologen derivatives, β-nicotinamide adenine dinucleotide-reduced dipotassium salt, and poly(ethyleneimine) were used as n-type dopants in which electrons were donated from adsorbates to CNTs.[11−14] The direction of electron transfer is generally determined by the redox potential difference between the CNTs and adsorbates. The redox potentials have been derived for nanotubes with different diameters and chiralities.[15] Because nanotubes have van Hove singularities (VHSs) in the valence and conduction band due to their one-dimensional nature, extraction of electrons from CNTs or donation of electrons to CNTs does not occur continuously.[15,16]

For instance, a typical strong p-dopant, Au^{3+}, has a reduction potential of 1.5 V with regard to a normal hydrogen electrode. This value is greater than the first and second VHSs in the valence bands for CNTs with diameters ranging from 1.0 to 1.5 nm, typical for arc discharge samples.[17] Therefore, the first and second VHS electrons in the semiconducting nanotubes are extracted to reduce Au^{3+}. The Au^{3+} ions are sufficiently strong dopants to remove the first VHS in metallic nanotubes. As a result, the VHS-related absorption peaks are suppressed.[11]

*Address correspondence to jingkong@mit.edu, leeyoung@skku.edu.

Received for review October 22, 2010 and accepted December 23, 2010.

Published online January 05, 2011
10.1021/nn1028532

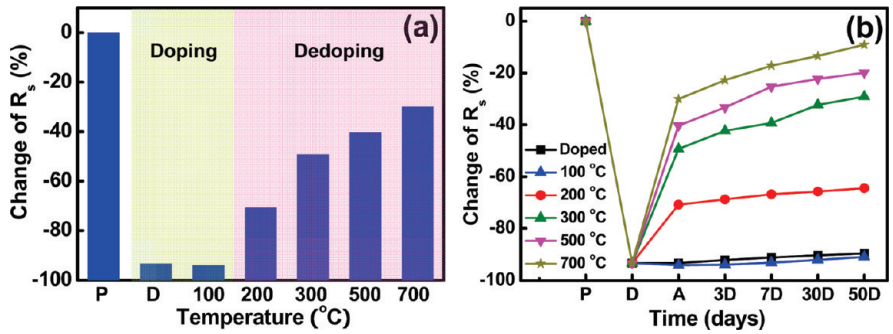

Figure 1. (a) The change in sheet resistance with doping. The change in sheet resistance was defined according to 100(R_s − R_{si})/R_{si}, where R_s is the measured sheet resistance and R_{si} is the initial sheet resistance of the pristine sample. The doped sample was further annealed at different temperatures for 1 h under an Ar ambient. (b) Aging of samples with thermal annealing for up to 50 days (lines for guideline): (P) pristine, (D) doped, (A) annealed, (*n*D) *n* days.

The strong charge transfer was also observed in Raman spectra as a blueshift of the G-band peak and suppression of the electron−phonon interaction in the lower energy side of the G-band.[11] Gold ions are usually obtained by dissolving $AuCl_3$ powder in nitromethane or deionized water.[10,11,15] It is believed that Au^{3+} ions in solution play a key role in the extraction of electrons from CNTs. It has been recently proposed that Au^{3+} ions theoretically act as a precursor for further Cl adsorption in which the chemisorbed Cl ions extract electrons directly from CNTs.[18]

The purpose of this paper is to investigate the roles of Au cations and Cl anions in solution in CNT doping. In this study, single walled carbon nanotubes (SWCNTs) were sprayed onto quartz film to form a thin film and were further doped with $AuCl_3$ solution in nitromethane. The samples were annealed at various temperatures under an Ar atmosphere in order to observe the effect of Cl atoms. The presence of Cl atoms was observed using XPS. At 500 °C, Cl atoms were completely desorbed from CNTs, and the sheet resistance was increased by 40% compared to that of the pristine doped film. This implies that Cl rather than Au cations adsorption plays an important role in CNT doping, congruent with theoretical predictions.[18]

RESULTS AND DISCUSSION

Changes in Sheet Resistance with Doping and Annealing. Figure 1a shows the change in sheet resistance as a function of annealing temperature. The sheet resistance was normalized with respect to the pristine sample in order to avoid ambiguity of the pristine SWCNT films that had slightly different sheet resistances. The pristine SWCNTs typically had a sheet resistance of approximately 600 Ω/sq at a transmittance of 85%. By simply spin-casting the $AuCl_3$ solution onto the SWCNT film, the sheet resistance was reduced by 94% compared to that of the pristine film. This significant drop in sheet resistance was interpreted as an extraction of electrons from CNTs due to the reduction of Au^{3+} to Au^0 so that p-type doping or hole doping was invoked and the hole carriers concentration was increased.[11] Annealing this sample at 100 °C under an Ar ambient slightly decreased the sheet resistance. The dedoping effect was observed with 200 °C annealing by increasing the sheet resistance to 70%. The sheet resistance increased further as the temperature increased. At 500−700 °C annealing, Cl atoms were completely desorbed, and the sheet resistance was reduced only 30−40% compared to that of the pristine sample. Therefore, 60−70% of the sheet resistance change was attributed to the Cl atoms.

TABLE 1. The Change in the Sheet Resistance Relative to That of the Original Undoped Pristine Sample after 50 days (%) at Different Annealing Temperatures

condition	100 °C	200 °C	300 °C	500 °C	700 °C
after annealing	−94.1	−70.8	−49.3	−40.3	−30.0
after 50 days	−90.9	−64.5	−29.1	−19.9	−9.1
difference	3.2	6.3	20.0	20.4	20.9

The films annealed after doping were exposed to ambient conditions for up to 50 days in order to test the environmental stability, as shown in Figure 1b. Annealing at temperatures up to 200 °C showed no significant change in the sheet resistance (see Table 1). This indicates that environmental stability was well maintained during heating up to 200 °C. However, the dedoping effect or increase in sheet resistance becames more prominent at higher annealing temperatures (300−700 °C), and the sheet resistance increased gradually with aging, reaching approximately 20% after 50 days. This environmental instability originates from the desorption of chlorine atoms and the readsorption of moisture molecules from the surrounding air.

Raman Spectroscopy at Different Annealing Temperatures. To investigate the p-doping behavior, the SWCNT films were characterized using Raman spectroscopy with a laser excitation energy of 1.96 eV. In general, the doping phenomena in Raman spectra is estimated by the shift in the G-band peak position near 1590 cm^{-1} due to charge transfer,[11,19] the change in the Breit−Wigner−Fano (BWF) shape near 1545 cm^{-1} due to the

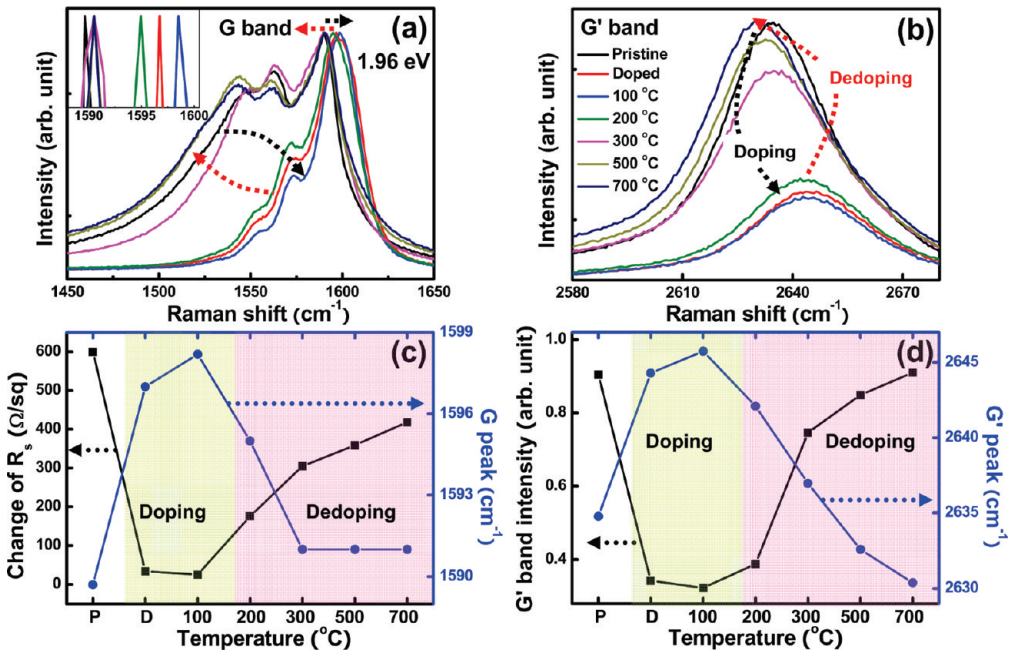

Figure 2. (a) G-band and (b) G′-band in the Raman spectra of the doped SWCNT film after annealing at different temperatures. The inset shows the peak position shift. (c) The relationship between sheet resistance and G-band peak position and (d) the relationship between G′-band intensity and G′-band peak position at an excitation energy of 1.96 eV.

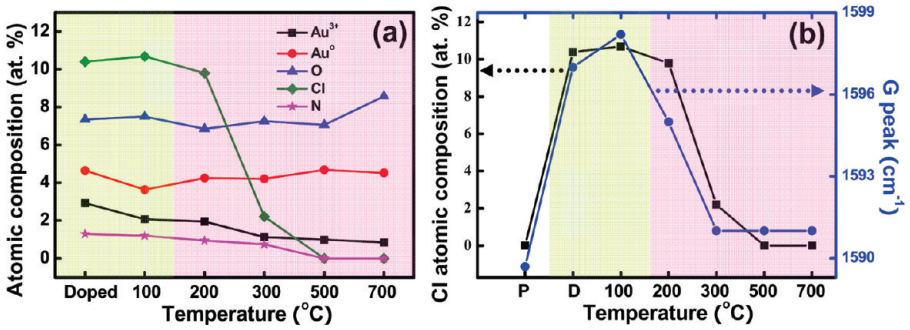

Figure 3. (a) Compositional changes in various atoms extracted from the fitting of the related XPS peaks at different annealing temperatures. (b) The relationship between chlorine composition and G-band peak position.

phonon stiffening/softening,[20,21] and the intensity change in the G′ band near 2700 cm^{-1} due to the change of the metallicity of the CNTs.[22] The G-band peak position shifted to 1597 from 1590 cm^{-1} with doping (Figure 2a). The slight upshift of the G-band peak by 1 cm^{-1} in the case of 100 °C annealing was also consistent with the slight decrease in the sheet resistance, as shown in Figure 2c. Alternatively, G-band peaks were downshifted with high temperature annealing at 300−700 °C, reaching nearly the same level as that of the pristine sample.

The BWF line was significantly reduced with doping and recovered to a similar level to the pristine sample after high temperature annealing (Figure 2a). The G-band and G′-band peak positions were upshifted in congruent with the previous reports.[11,22,29] It is also intriguing to observe that the changes in the peak intensities are inversely proportional to those of peak positions as shown in Figure 2b,d.[22] The G′ band intensity was normalized with respect to the G band intensity for all the samples in this work. All of these changes in the Raman spectra were simply an indication of the doping and dedoping phenomena related to the creation or annihilation of CNT hole carriers. The change in the sheet resistance was inversely proportional to the change in the G-band peak position, as shown in Figure 2c.

XPS Analysis of the Doping/Dedoping Mechanism. Although the change in the sheet resistance and peak changes of the G- and G′-bands in Raman spectroscopy with respect to annealing temperature were corroborated experimentally, the origins of such changes remain unclear. The samples at different annealing temperatures were characterized using XPS (see Supporting Information S1). The atomic compositions of Au^{3+}, Au^{0}, Cl, O, and N were determined by fitting each core level spectra (Figure 3a and Table 2). The presence of the Cl peak with a relatively high composition greater than 10%, the most prominent peak among

TABLE 2. The Compositional Changes in Au^{3+}, Au^0, and Cl Obtained from the Fitting of the Related XPS Peaks with Various Annealing Temperatures

	Au 4f fitting binding energy (eV) (relative atomic percentage %)			Cl 2p fitting binding energy (eV) (relative atomic percentage %)		
condition	Au^0 $4f_{7/2}$	Au^0 $4f_{5/2}$	Au^{3+} $4f_{7/2}$	Au^{3+} $4f_{5/2}$	Cl $2p_{3/2}$	Cl $2P_{1/2}$
doped	84.7	88.4	86.6	90.6	198.4	200.1
	(2.01%)	(2.63%)	(1.40%)	(1.52%)	(4.28%)	(6.11%)
100 °C	84.6	88.2	86.8	90.7	198.3	200.7
	(1.73%)	(1.90%)	(0.63%)	(1.43%)	(4.08%)	(6.60%)
200 °C	84.5	88.2	86.3	90.2	198.2	200.6
	(1.93%)	(2.31%)	(0.93%)	(1.01%)	(3.33%)	(6.50%)
300 °C	84.2	87.8	85.7	89.3	198.0	200.2
	(2.11%)	(2.09%)	(0.50%)	(0.62%)	(0.75%)	(1.40%)
500 °C	84.1	87.7	85.6	89.3		
	(2.31%)	(2.37%)	(0.50%)	(0.49%)	(0%)	(0%)
700 °C	84.0	87.7	85.5	89.3		
	(2.26%)	(2.35%)	(0.41%)	(0.43%)	(0%)	(0%)

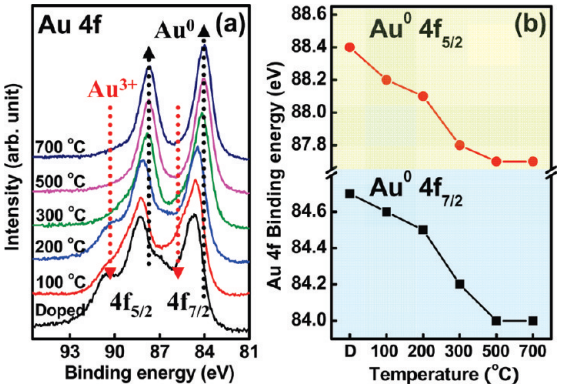

Figure 4. (a) The change in the Au 4f core level as a function of the annealing temperature. (b) The peak position of the Au 4f core level is shown as a function of the annealing temperature. The position is related to the Au cluster size.

the adsorbate peaks, clearly implies the presence of Cl atoms on the CNT surface. The proportion of Cl atoms was slightly increased at 100 °C annealing, congruent with the slight reduction in the sheet resistance (Figure 1a). This small increase in the relative proportion of Cl atoms is attributed to desorption of adsorbates that are physisorbed to the CNT surface. With increasing annealing temperature, the Cl proportion decreased rapidly, and Cl atoms were completely removed at 500 °C. This implies that Cl atoms were strongly chemisorbed onto the CNT surface. It has been proposed that the positively charged CNTs due to Au^{3+} cation adsorption induce Cl^- anion adsorption, resulting in the formation of a strong chemical bond between Cl and the CNT surface.[18] It is also expected that electrons can be extracted from CNTs due to the higher electronegativity of the Cl atom compared to that of the carbon atom. This was again confirmed through a strong correlation between the change in the Cl composition and the G-band peak shift (Figure 3b).

One intriguing issue associated with Cl adsorption is the hygroscopic effect or moisture-favorable effect.[18,23] At low temperature annealing, Cl remained unchanged on the CNT surface. Since Cl atoms are associated with moisture, no further adsorption of environmental adsorbates is induced and high environmental stability is maintained, as shown in Figure 1b. However, at higher temperatures, the Cl atoms and environmental adsorbates were desorbed. As a consequence, the sheet resistance increased and the environmental stability was not maintained due to further continuous adsorption of environmental gases. The compositional changes in the numerical data are provided in Table 2.

TEM Observations of the Au^0 Cluster Formation. Another intriguing change to note is the compositional change in Au^{3+} ions. The composition of Au^{3+} cations was gradually reduced up to 300 °C and was saturated at higher temperatures, whereas the Au^0 composition was conversely altered. The gradual decrease in Au^{3+} ions indicates that Au^{3+} ions were further reduced to Au^0 due to transformation of the unstable Au^{3+} in $AuCl_4^-$ to a stable Au^0 cluster during Cl desorption and/or the presumed desorption of Au^{3+} cations during annealing.[24] Transformation of the Au^{3+} peak to Au^0 is clearly shown in Figure 4a. The Au^{3+} peaks near 90.5 eV in Au $4f_{5/2}$ and near 86.0 eV in Au $4f_{7/2}$ were diminished with increasing temperature. Figure 4b shows the peak shift of Au^0, in which the peak energy continued to decrease as the annealing temperature increased, implying an increase in Au^0 cluster sizes.[25] To confirm this, TEM images were taken, as shown in Figure 5. Small-size Au clusters with an average size of 7 nm were visible in the doped sample. The sizes of the Au^0 clusters increased with increasing annealing temperature, with the Au nanoparticles reaching a size of 32 nm at 700 °C (Table 3). The melting temperature of Au nanoparticles strongly relies on their diameters owing to the surface free energy of the particle, which induces a size dependence of the chemical potentials.[26] This is well established by Pawlow's theory:

$$\frac{T_m(r)}{T_m(\infty)} = 1 - \frac{4}{\rho_s L}\left\{\gamma_s - \gamma_l\left(\frac{\rho_s}{\rho_l}\right)^{2/3}\right\}\frac{1}{d}$$

where T_m is the melting temperature, ρ is a mass density, γ is the surface free energy, L is the molar heat of fusion, and d is the particle diameter. The parameter values used in this study were provided by Buffat and Borel (ρ_s and ρ_l = 19 and 17.3 g cm^{-3} for the solid (s) and liquid (l), respectively; γ_s and γ_l = 0.9 × 10^3 and 0.74 × 10^3 erg cm^{-2}, respectively; L = 5.38 × 10^8 erg g^{-1}), where ∞ signifies the bulk material. According to this formula, Au nanoparticles with sizes smaller than 3 nm should melt at 500 °C. In other words, small Au nanoparticles were expected to be melted easily within our experimental temperature range, allowing them to be incorporated into larger particles to form larger Au nanoparticles.

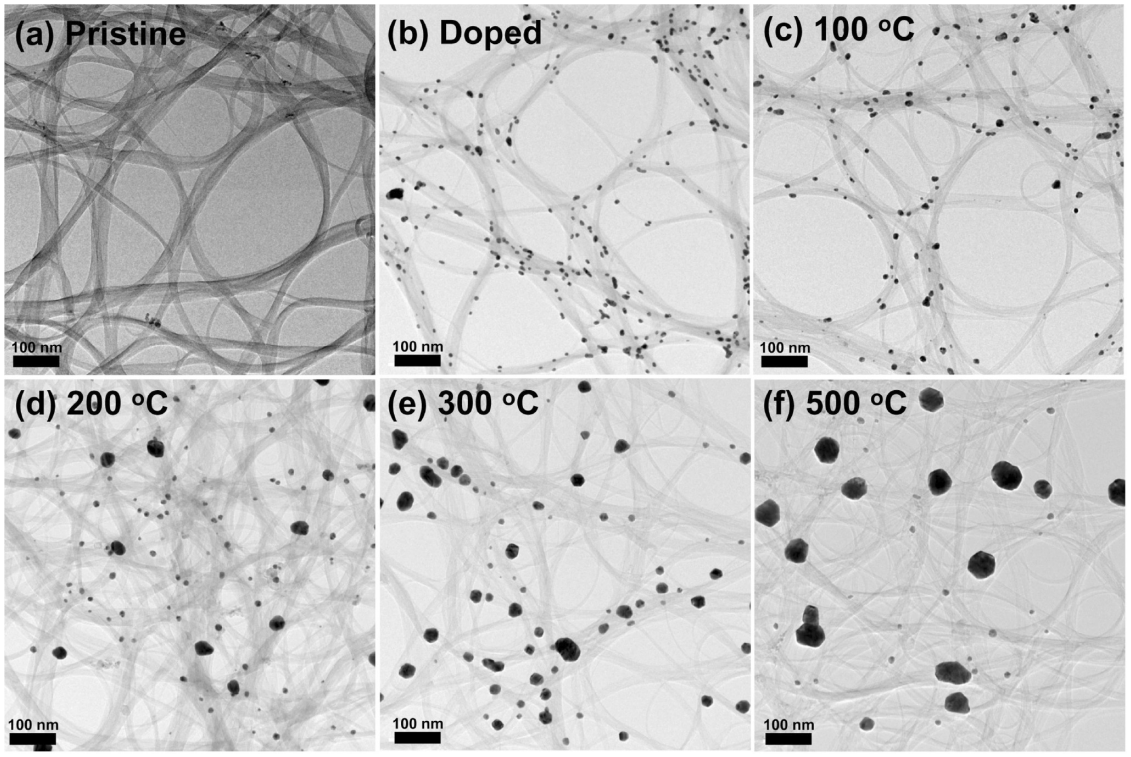

Figure 5. TEM images of the related SWCNT films at various conditions: (a) pristine, (b) doped, (c) annealed at 100 °C, (d) annealed at 200 °C, (e) annealed at 300 °C, and (f) annealed at 500 °C after doping. The scale bar is 100 nm.

TABLE 3. Gold Size Distribution at Different Temperature Conditions

condition	doped	100 °C	200 °C	300 °C	500 °C
size (SD) (nm)[a]	7 (2)	8 (2)	11(3)	23 (18)	32 (23)

[a] SD: standard deviation.

Proposed Cl-Associated Doping/Dedoping Mechanism. When $AuCl_3$ is dissolved in a solvent, different ionic conformation can be formed depending on the amount of the coordinating agent. Water or acetonitrile preferentially leads to a square planar geometry of $AuCl_4^-$.[24] In this study, we used nitromethane, a poor coordinating solvent. It was understood that the following reactions would occur in a manner similar to graphene doping:[27]

Step 1: Ionization of CNTs and Reduction of Au^{3+} to Au^0

$$2CNT + 2AuCl_3 \rightarrow 2CNT^+ + AuCl_2^- (Au\ I) + AuCl_4^- (Au\ III) \quad (1)$$

$$3AuCl_2^- \rightarrow 2Au^0\downarrow + AuCl_4^- (Au\ III) + 2Cl^- \quad (2)$$

$$AuCl_4^- + 3CNT \rightarrow 3CNT^+ + Au^0 + 4Cl^- \quad (3)$$

The uncoordinated $AuCl_2^-$ (Au I) easily disproportionates due to its instability to form $AuCl_4^-$ (Au III), Au^0, and Cl^-. (Au I) and (Au III) symbolize coordinated ions with nitromethane solvent, which are not completely ionized. CNTs could be p-doped *via* reactions 1−3. The doping is progressed further *via* a neutralization process of charged CNTs with Cl ions. CNTs are more heavily doped by donating electrons to Cl^-:

Step II: Neutralization of CNTs by Cl Anions

$$CNT^+ + Cl- \rightarrow CNT-Cl \quad (4)$$

or

$$CNT^+ + AuCl_4^- \rightarrow CNT-AuCl_4 \quad (5)$$

With annealing at high temperature or dedoping, Cl atoms can be detached directly from the CNT surface or the Cl atom in the $AuCl_4$ cluster can be partially detached.

Step III: Desorption of Cl Atoms and Dedoping Process

$$2CNT-Cl \rightarrow 2CNT + Cl_2\uparrow \quad (6)$$

$$CNT-AuCl_4 \rightarrow CNT-Au + 2Cl_2\uparrow \quad (7)$$

Reactions 6 and 7 are the reverse reactions of 4 and 5. Since the desorption process occurs due to high temperature annealing, Cl gas is formed and evaporates. Therefore, a lower doping effect in CNT is expected due to the removal of a high electronegative Cl species. During this desorption process, Cl or $AuCl_4$ can still be attached to the CNT at low temperature, although Cl is completely desorbed at high temperature annealing. In high temperature annealing, Au^0 atoms are attached to the CNT surface and agglomerate to form large clusters. CNT−Au is still retained, even in high temperature annealing, and contributes to a 30% reduction in the sheet resistance compared to that of the pristine sample. The related

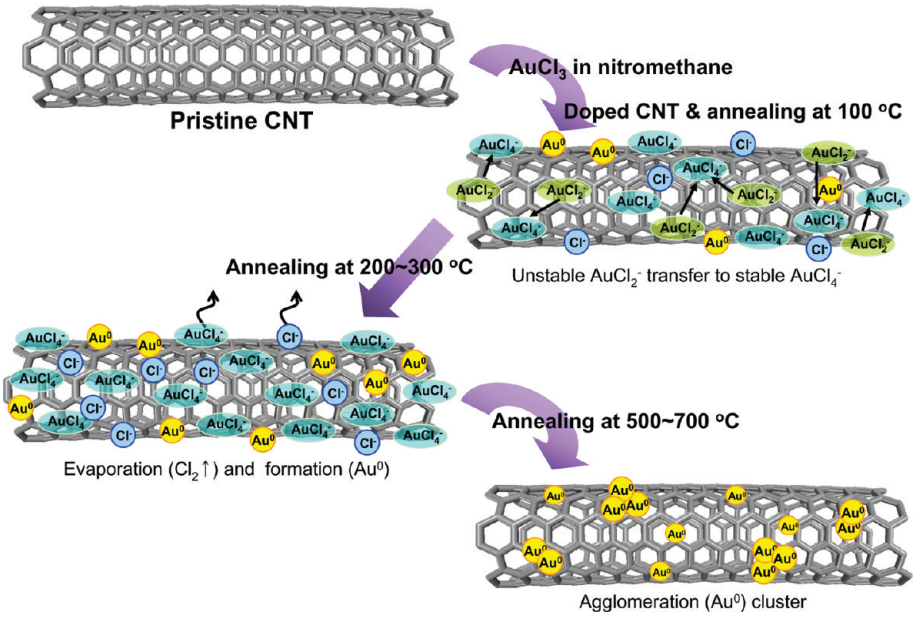

Figure 6. Cl-associated doping/dedoping mechanism.

schematic for the Cl-associated doping/dedoping mechanism is shown in Figure 6.

CONCLUSION

We have investigated the role of Au cations and Cl anions in solution for $AuCl_3$ doping on CNTs. We found that the doping level of the CNT films is strongly correlated with the amount of adsorbed Cl anions, which was confirmed by the sheet resistance change and the peak shift of XPS and Raman spectra. This is in contrast to the general belief that only Au^{3+} reduction to neutral Au^0 plays a role in CNT doping. To confirm this doping mechanism, the CNT film was heat-treated as a function of annealing temperature (100−700 °C) under Ar ambient. Cl adsorption plays more important role in doping CNTs, while the reduction of Au^{3+} to Au^0 plays a role as an intermediate precursor to accommodate subsequent Cl adsorption. The analysis was in good agreement with the previous theoretical prediction.

EXPERIMENTAL SECTION

Film Preparation. Purified arc-discharge SWCNTs (Iljin Nanotech Co., Ltd., purity, 93%) with a mean diameter of 1.5 nm (range, 1.2−1.8 nm) and a typical length of a few micrometers were used in this experiment. The SWCNTs (2 mg) were added to 30 mL of 1,2-dichloroethane (DCE: anhydrous, 99.8% Sigma-Adrich) followed by sonication in a bath type sonicator (RK 106, Bandelin Electronic, Berlin, Germany) for 6 h.[28] The solution was centrifuged (Hanil Science Industrial Co., Ltd., Mega 17R) at 8000 rpm for 10 min. The supernatant of the resulting solution was sprayed onto a quartz substrate (2×2 cm^2) with an Ar gas brush pistol (Gunpiece GP-1, Fuso Seiki Co., Ltd.) and was further heat-treated at 900 °C for 1 h under an Ar atmosphere to avoid the solvent effect.[29] This sample was assigned as the pristine sample.

Doping and Annealing Procedure. Gold trichloride ($AuCl_3$: purity 99%, Sigma-Aldrich) powder was used in this study. The powder was dissolved in nitromethane (Sigma-Aldrich) to a concentration of 20 mM. One 400 μL drop of the doping solution was placed onto the SWCNT film. After a residual time of 30 s, the solvent was spin-coated at 2500 rpm for 1 min (Midas System, Spin 2000). The film was exposed to ambient conditions for several hours prior to analysis. To investigate the effects of chlorine on the doped-CNT film, the CNT film after doping was annealed at different temperatures under an Ar atmosphere. The CNTs were not damaged at annealing temperatures up to 500 °C. The sheet resistance of the CNT film was evaluated for up to 50 days to evaluate the stabilities of CNT films under ambient conditions.

Film Measurements and Electrical Characterization. The sheet resistance was measured at room temperature using a four-point method (Keithley 2000 multimeter). Raman spectroscopy (Renishaw, RM-1000 Invia) with an excitation energy of 1.96 eV (632.8 nm, He−Ne laser) was used to characterize the optical properties of doped SWCNTs. X-ray photoelectron spectroscopy (XPS, ESCA2000, VG Microtech, England) was performed to determine the presence of residual material and the degree of doping. HR-TEM (JEM 2100F, JEOL) was used to investigate the Au particle after annealing at different conditions.

Supporting Information Available: The XPS spectra of doped CNT samples at different annealing temperatures. This material is available free of charge *via* the Internet at http://pubs.acs.org.

Acknowledgment. This study was supported by the STAR-faculty program and WCU (World Class University) program through the KRF funded by the MEST (R31-2008-000-10029-0), the Industrial Technology Development Program (10031734) of the Ministry of Knowledge Economy (MKE), and the IRDP of NRF (2010-00429) through a grant provided by MEST in 2010 in Korea. S.M.K. acknowledges the Seoul Science Fellowship.

REFERENCES AND NOTES

1. Tans, S. J.; Verschuerene, A. R. M.; Dekker, C. Room-Temperature Transistor Based on a Single Carbon Nanotube. *Nature* **1998,** *393*, 49–52.

2. Durkop, T.; Getty, S. A.; Cobas, E.; Fuhrer, M. S. Extraordinary Mobility in Semiconducting Carbon Nanotubes. *Nano Lett.* **2004,** *4*, 35–39.
3. Zhou, C.; Kong, J.; Yenilemez, E.; Dai, H. Modulated Chemical Doping of Individual Carbon Nanotubes. *Science* **2000,** *290*, 1552–1555.
4. Javey, A.; Tu, R.; Farmer, D. B.; Guo, J.; Gordon, R. G.; Dai, H. High Performance n-Type Carbon Nanotube Field-Effect Transistors with Chemically Doped Contacts. *Nano Lett.* **2005,** *5*, 345–348.
5. Stephan, O.; Ajayan, P. M.; Colliex, C.; Redlich, Ph.; Lambert, J. M.; Bernier, P.; Lefin, P. Doping Graphitic and Carbon Nanotube Structures with Boron and Nitrogen. *Science* **1994,** *266*, 1683–1685.
6. Derycke, V.; Martel, R.; Appenzeller, J.; Avouris, Ph. Controlling Doping and Carrier Injection in Carbon Nanotube Transistors. *Appl. Phys. Lett.* **2002,** *80*, 2773–2775.
7. Bockrath, M.; Hone, J.; Zettl, A.; McEuen, P. L.; Rinzler, A. G.; Smalley, R. E. Chemical Doping of Individual Semiconducting Carbon-Nanotube Ropes. *Phys. Rev. B* **2000,** *61*, R10606–R10608.
8. Derycke, V.; Martel, R.; Appenzeller, J.; Avouris, Ph. Carbon Nanotube Inter- and Intramolecular Logic Gates. *Nano Lett.* **2001,** *1*, 453–456.
9. Jang, J. H.; Lim, S. C.; Duong, D. L.; Kim, G.; Yu, W. J.; Han, K. H.; Min, Y. −S.; Lee, Y. H. Doping of Carbon Nanotubes Using Low Energy Ion Implantation. *J. Nanosci. Nanotechnol.* **2010,** *10*, 3934–3939.
10. Choi, H. C.; Shim, M.; Bangsaruntip, S.; Dai, H. Spontaneous Reduction of Metal Ions on the Sidewalls of Carbon Nanotubes. *J. Am. Chem. Soc.* **2002,** *124*, 9058–9059.
11. Kim, K. K.; Bae, J. J.; Park, H. K.; Kim, S. M.; Geng, H. −Z.; Park, K. A.; Shin, H. −J.; Yoon, S. −M.; Choi, J. −Y.; Lee, Y. H. Fermi Level Engineering of Single-Walled Carbon Nanotubes by $AuCl_3$ Doping. *J. Am. Chem. Soc.* **2008,** *130*, 12757–12761.
12. Kim, S. M.; Jang, J. H.; Kim, K. K.; Park, H. K.; Bae, J. J.; Yu, W. J.; Lee, I. H.; Kim, G.; Duong, D. L.; Kim, U. J.; *et al*. Reduction-Controlled Viologen in Bisolvent as an Environmentally Stable n-Type Dopant for Carbon Nanotubes. *J. Am. Chem. Soc.* **2009,** *131*, 327–331.
13. Kang, B. R.; Yu, W. J.; Kim, K. K.; Park, H. K.; Kim, S. M.; Park, Y.; Kim, G.; Shin, H. -J.; Kim, U. J.; Lee, E. -H.; *et al.* Restorable Type Conversion of Carbon Nanotube Transistor Using Pyrolytically Controlled Antioxidizing Photosynthesis Coenzyme. *Adv. Funct. Mater.* **2009,** *19*, 2553–2559.
14. Shim, M.; Javey, A.; Kam, N. W. S.; Dai, H. Polymer Functionalization for Air-Stable n-Type Carbon Nanotube Field-Effect Transistors. *J. Am. Chem. Soc.* **2001,** *123*, 11512–11513.
15. Kim, K. K.; Yoon, S. -M.; Park, H. K.; Shin, H. −J.; Kim, S. M.; Bae, J. J.; C, Y.; Kim, J. M.; Choi, J. −Y.; Lee, Y. H. Doping Strategy of Carbon Nanotubes with Redox Chemistry. *New J. Chem.* **2010,** *34*, 2183–138.
16. An, K. H.; Lee, Y. H. Electronic-Structure Engineering of Carbon Nanotubes. *NANO* **2006,** *1*, 115–138.
17. Kataura, H.; Kumazawa, Y.; Maniwa, Y.; Umezu, I.; Suzuki, S.; Ohtsuka, Y.; Achiba, Y. Optical Properties of Single-Wall Carbon Natnobues. *Synth. Met.* **1999,** *103*, 2555–2558.
18. Duong, D. L.; Lee, I. H.; Kim, K. K.; Kong, J.; Lee, S. M.; Lee, Y. H. Carbon Nanotube Doping Mechanism in a Salt Solution and Hygroscopic Effect: Density Functional Theory. *ACS Nano* **2010,** *4*, 5430–5436.
19. Dresselhaus, M. S.; Dresselhaus, G.; Saito, R.; Jorio, A. Raman Spectroscopy of Carbon Nanotubes. *Phys. Rep.* **2005,** *409*, 47–99.
20. Brown, S. D. M.; Jorio, A.; Corio, P.; Dresselhaus, M. S.; Dresselhaous, G.; Saito, R.; Kneipp, K. Origin of the Breit−Wigner−Fano Lineshape of the Tangential G-band Feature of Metallic Carbon Nanotubes. *Phys. Rev. B* **2001,** *63*, 155414/1–8.
21. Rao, A. M.; Eklund, P. C.; Bandow, S.; Thess, A.; Smalley, R. E. Evidence for Charge Transfer in Doped Carbon Nanotube Bundles from Raman Scattering. *Nature* **1997,** *388*, 257–259.
22. Kim, K. K.; Park, J. S.; Kim, S. J.; Geng, H. −Z.; An, K. H.; Yang, C. −M.; Sato, K.; Saito, R.; Lee, Y. H. Dependence of Raman Spectra G′ band Intensity on Metallicity of Single-Wall Carbon Nanotubes. *Phys. Rev. B* **2007,** *76*, 205426/1–8.
23. Lee, I. H.; Kim, U. J.; Son, H. B.; Yoon, S. -M.; Yao, F.; Yu, W. J.; Duong, D. L.; Choi, J. -Y.; Kim, J. M.; Lee, E. H.; Lee, Y. H. Hygroscopic Effects on $AuCl_3$-Doped Carbon Nanotubes. *J. Phys. Chem. C.* **2010,** *114*, 11618–11622.
24. Abdou, M. S. A.; Holdcroft, S. Oxidation of π-Conjugated Polymers with Gold Trichloride: Enhanced Stability of the Electronically Conducting State and Electroless Deposition of Au^0. *Synth. Met.* **1993,** *60*, 93–96.
25. Reinke, P.; Howe, J.; Eswaramoorthy, S. Understanding the Role of Annealing Temperature and Ion Energy in the Growth of Au Clusters. *J. Appl. Phys.* **2006,** *100*, 024303/1–6.
26. Dick, K.; Dhanasekaran, T.; Zhang, Z.; Meisel, D. Size-Dependent Melting of Silica-Encapsulated Gold Nanoparticles. *J. Am. Chem. Soc.* **2002,** *124*, 2312–2317.
27. Kim, K. K.; Reina, A.; Shi, Y.; Park, H.; Li, L. −J.; Lee, Y. H.; Kong, J. Enhancing the Conductivity of Transparent Graphene Films *via* Doping. *Nanotechnology*. **2010,** *21*, 285205/1–6.
28. Kim, K. K.; Bae, D. J.; Yang, C. −M.; An, K. H.; Lee, J. Y.; Lee, Y. H. Nanodispersion of Single-Walled Carbon Nanotubes Using Dichloroethane. *J. Nanosci. Nanotechnol.* **2005,** *5*, 1055–1059.
29. Shin, H. -J.; Kim, S. M.; Yoon, S. -M.; Benayad, A.; Kim, K. K.; Kim, S. J.; Park, H. K.; Choi, J. −Y.; Lee, Y. H. Tailoring Electronic Structures of Carbon Nanotubes by Solvent with Electron-Donating and -Withdrawing Groups. *J. Am. Chem. Soc.* **2008,** *130*, 2062–2066.